A Simple Layer-by-Layer Assembly Strategy for a Reagentless Biosensor Based on a Nanocomposite of Methylene Blue-Multiwalled Carbon Nanotubes

Yiming Zhang, *Lijun Liu*, *Fengna Xi*, *Tianxing Wu*, *Xianfu Lin**

Department of Chemistry, Zhejiang University, Hangzhou 310027, P. R. China
*e-mail: llc123@zju.edu.cn

Received: June 16, 2009
Accepted: September 12, 2009

Abstract
A simple layer-by-layer (LBL) assembly strategy was established for constructing a novel reagentless biosensor based on a nanocomposite of methylene blue multiwalled carbon nanotubes (MB-MWNTs). A nanocomposite of MB-MWNTs was obtained by direct premixing and possessed good dispersion in barbital-HCl buffer. Through electrostatic interactions, the nanocomposite of MB-MWNTs could alternately be assembled with horseradish peroxidase (HRP) on the Au electrode modified with precursor films. UV/Vis spectra and scanning electron microscopy (SEM) were applied to reveal the formation of the nanocomposite of MB-MWNTs. The LBL assembly process was also verified by electrochemical impedance spectroscopy (EIS). The MB is a well-established mediator and efficiently facilitated the electron shuttle between the HRP and the electrode, as demonstrated by the cyclic voltammetry (CV) measurements. The as-prepared reagentless biosensor exhibited a fast response for the determination of hydrogen peroxide (H_2O_2) and reached 95% of the steady-state current within 3 s. It was found that the linear response range of the reagentless biosensor for H_2O_2 was from 4.0 μM to 3.78 mM with a detection limit of 1.0 μM and a sensitivity of 22.5 μA mM^{-1}. The biosensor exhibited a high reproducibility and stability.

Keywords: Multiwalled carbon nanotubes, Reagentless biosensor, Layer-by-layer assembly, Methylene blue, Hydrogen peroxide, Nanotubes, Biosensors

DOI: 10.1002/elan.200900307

1. Introduction

The accurate determination of hydrogen peroxide (H_2O_2) is important in chemical, biological, environmental and clinical fields. Compared with conventional detection methods, such as UV/Vis spectrophotometry [1] and chemiluminescence [2], an amperometric biosensor is particularly suited for the analysis of H_2O_2 due to its simplicity and high sensitivity [3, 4]. The construction of sensitive amperometric biosensors is an attractive goal.

Reagentless biosensors created by co-immobilization of electron mediators together with enzymes on the electrode surfaces were effective in improving the performance of amperometric biosensors. These sensors were able to facilitate the electron shuttle between the active center of the enzyme and the surface of the electrode [5–9]. Methylene blue (MB) is a typical cationic organic dye, and it is a well-established electron mediator. Therefore, MB-modified electrodes are attractive for reagentless biosensors [10]. Several strategies to immobilize mediators have been proposed to fabricate reagentless biosensors. Direct dropping or adsorption of electron mediators on the surface of the electrode are simple methods [11, 12]. To further improve the stability and performance of the biosensor, it will be significant to propose new way to fabricate reagentless biosensor.

Recently, carbon nanotubes (CNTs) were employed to fabricate biosensors due to their high surface-to-volume ratio, unique mechanical properties and high chemical stability. When CNTs were used as matrices, enzymes or proteins could be effectively immobilized, and the performance of the prepared biosensor could be enhanced [13, 14]. Fabricating nanocomposites of electron mediators and CNTs would be an effective way to construct reagentless biosensors [5, 7, 15]. In the case of biosensors based on MB-CNTs, MB could be used as a mediator for electron transfer, and CNTs served as excellent conductors and matrices for enzyme immobilization. Therefore, the synergistic effects of the CNTs and mediators could produce sensitive reagentless biosensors. Thus, finding a simple and effective approach to fabricate nanocomposites of MB-MWNTs to construct reagentless biosensors is of great significance.

LBL assembly has been proven as simple and versatile for the preparation of stable ultrathin multilayer films. It is based on the alternate assembly of polyelectrolytes, nanomaterials and proteins [16, 17]. Moreover, LBL films can provide suitable microenvironments to retain the activity of biomolecules due to their mild conditions [18–20]. Recently, there have been many reports about LBL assembly of MWNTs and polyelectrolytes with enzymes. The fabricated

biosensors that were tested exhibited good performance when sensing different substrates [21–23].

This work proposes a simple LBL assembly strategy for constructing novel reagentless biosensors based on a nanocomposite of methylene blue multiwalled carbon nanotubes (MB-MWNTs). A nanocomposite of MB-MWNTs was obtained through a direct premixing procedure, and it possessed good dispersion in barbital-HCl buffer. The MB molecules with positive charge were stably anchored on the surface of the MWNTs due to electrostatic adsorption and $\pi-\pi$ stacking forces [5, 24]. Using horseradish peroxidase (HRP) as a model enzyme, the $(MB\text{-}MWNTs/HRP)_n$ multilayer was prepared on precursor films modified by Au electrodes through an electrostatic interaction. The fabricated nanocomposite of MB-MWNTs acted as an effective electron mediator, and the as-prepared reagentless biosensor could be used for the determination of H_2O_2. The resulting biosensor exhibited high reproducibility and stability.

2. Experimental

2.1. Chemicals and Materials

Multiwalled carbon nanotubes (95%, MWNTs) were purchased from Shenzhen Nanotech Port Co., Ltd (Shenzhen, P. R. China). The purification and carboxylation procedures of the MWNTs were performed according to our previous work [25]. Methylene blue (MB) was obtained from Shanghai reagent company (Shanghai, P. R. China). Horseradish peroxidase (HRP, E.C.1.11.1.7, 250 U mg^{-1}, p*I* 7.2) was purchased from Shanghai Sanjie biotechnology Co., Ltd (Shanghai, P. R. China). Poly(sodium-p-styrene-sulfonate) (PSS, average MW 70,000), 3-Mercapto-1-propanesulfonic acid, sodium salt (MPS) and poly(allylamine hydrochloride) (PAH, average MW 15,000) were purchased from Sigma-Aldrich. Other chemicals were of analytical grade and used as received. All solutions were prepared with doubly distilled water.

2.2. Preparation of MB-MWNTs Nanocomposite Suspension

The MB solution (0.04 M barbital-HCl buffer, pH 8.0) at a concentration of 2.0 mM was used for the preparation of a nanocomposite of MB-MWNTs through a premixing procedure. A total of 2.0 mg of MWNT was added into 4.0 mL of MB solution. The mixture was sonicated for 15 min and shaken for 1 h (200 rpm, 25 °C). The solution was sonicated again for 15 min and stood overnight. Next, it was sonicated again for 15 min before use. A well-dispersed nanocomposite of MB-MWNTs in suspension was obtained.

2.3. Pretreatment of Au Electrode and Silicon Wafer

The Au electrode was polished with emery paper and then polished with 1.0, 0.5 and 0.03 μm Al_2O_3 slurry successively until a mirror-like surface was obtained. Then it was sonicated in doubly distilled water for 5 min and immersed in freshly prepared 'piranha' solution (3:1 mixture of concentrated H_2SO_4 and 30% H_2O_2, v/v) for 30 min at 80 °C. Next, the electrode was rinsed with distilled water under sonication assistance for 5 min. The obtained electrode was transferred to the electrochemical cell for further cleaning using cyclic voltammetry between -0.2 and $+1.4$ V in a 0.2 M H_2SO_4 solution at a scan rate of 100 mV s^{-1} until a stable cyclic voltammogram profile was obtained. The silicon wafer (0.5 cm × 0.5 cm) was immersed for 30 min in freshly prepared 'piranha' solution at 80 °C, then rinsed with distilled water with sonication for 5 min and dried with a nitrogen stream. Using this procedure, the cleaned silicon wafer was obtained.

2.4. Assembly of Multilayer Film

The pretreated Au electrode was modified in 0.02 M MPS for 10 h, and then it was immersed into PAH and PSS solutions (1.0 mg mL^{-1} in Glycine–NaOH buffer containing 0.4 M NaCl, pH 11.0) for 20 min to form MPS/PAH/PSS precursors [25]. The MPS/PAH/PSS/PAH precursors were fabricated by dipping PAH/PSS precursor into PAH solution for 20 min. The precursors were then ready for $(MB/HRP)_n$ and $(MB\text{-}MWNTs/HRP)_n$ multilayer assemblies on the Au electrode. The cleaned silicon wafer was immersed in PAH solution to form PAH precursors and use in assembly of $(MWNTs/HRP)_n$ and $(MB\text{-}MWNTs/HRP)_n$. After each assembly step, the modified electrode and silicon wafer were thoroughly rinsed with doubly distilled water.

(MB-MWNTs/HRP) multilayers were obtained by dipping precursor coated Au electrodes and silicon wafers into MB-MWNT nanocomposite suspensions for 1 h. They were then dipped in 2.0 mg mL^{-1} HRP solution (barbital-HCl buffer, pH 6.8) for 40 min. This assembly cycle was repeated until the required $(MB\text{-}MWNTs/HRP)_n$ multilayers were obtained. After each assembly step, the modified electrode was carefully rinsed with doubly distilled water. Accordingly, the $(MWNTs/HRP)_n$ and $(MB/HRP)_n$ multilayers were prepared for comparison.

2.5. Characterizations and Electrochemical Measurements

The UV/Vis spectra of the MB solution, MWNT suspension and MB-MWNT nanocomposite suspension were measured with a Shimadzu UV-2550 spectrophotometer (Shimadzu, Japan). The morphology of the assembled multilayers was recorded using a Sirion-100 field-emitting scanning electron microscope (SEM, FEI, USA).

The electrochemical impedance spectroscopy (EIS), cyclic voltammetry (CV) and steady-state amperometric response experiments were performed with a CHI 650c electrochemical workstation (Shanghai CH Instrument Company, China). A conventional three-electrode system was used. Bare gold electrodes or modified gold electrodes were used as the working electrodes. The reference elec-

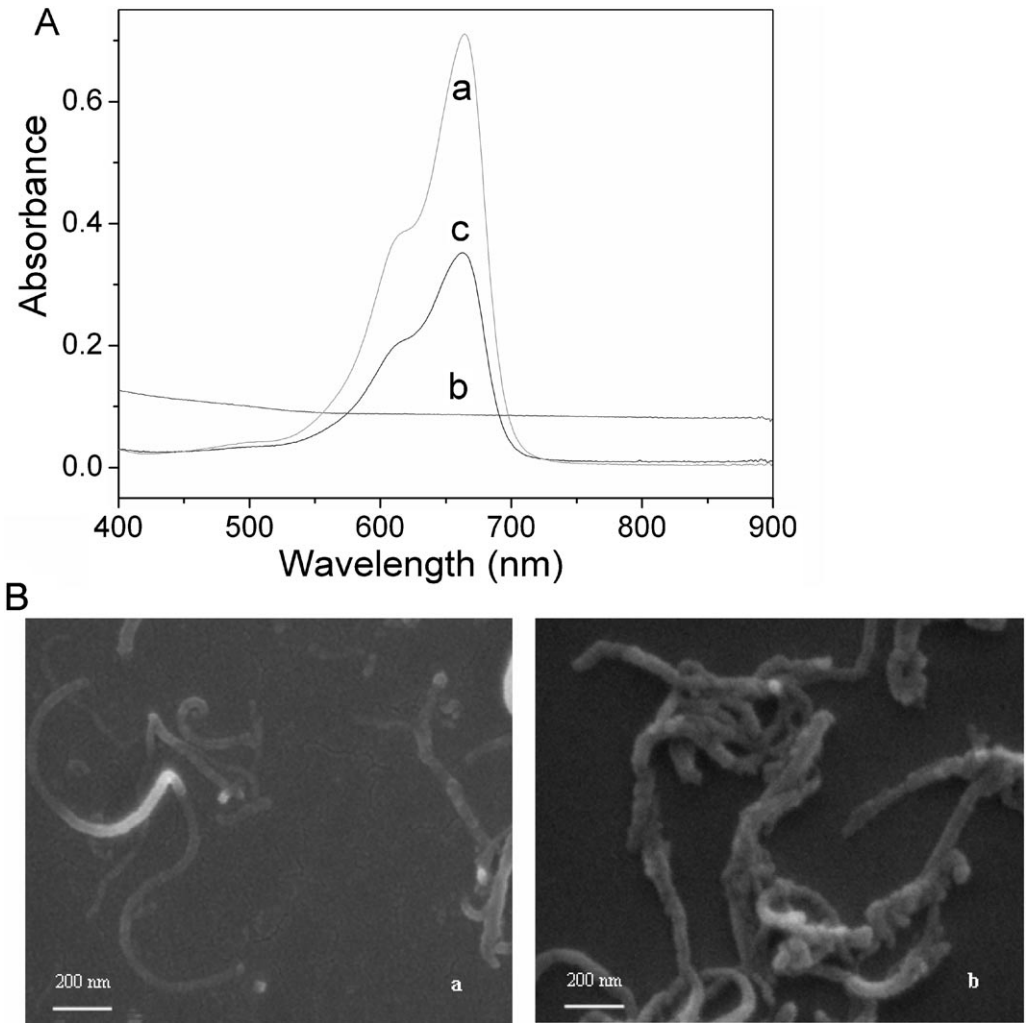

Fig. 1. A) UV/Vis spectra of a) 2 mM MB, b) 0.5 mg mL^{-1} MWNTs, and c) MB-MWNT nanocomposite suspension containing 0.5 mg mL^{-1} MWNTs and 2 mM MB, all in 0.04 M barbital-HCl buffer at pH 8.0. B) The SEM images of (a) MWNTs and (b) (MB-MWNTs) nanocomposite adsorbed onto silicon wafers.

trode was Ag/AgCl electrode (saturated with KCl), and a platinum disk was used as an auxiliary electrode. EIS was performed in a 5.0 mM $K_3Fe(CN)_6/K_4Fe(CN)_6$ (1:1) mixture with frequencies ranging from 10^4 to 10^{-1} Hz. A saturated calomel electrode (SCE) was used as the reference electrode for the EIS measurement. The CV and steady-state amperometric response experiments were performed in a phosphate buffer solution (0.1 M PBS, pH 6.8) as a supporting electrolyte. In the steady-state amperometric experiments, a typical steady-state response of the biosensor to successive injection of H_2O_2 was recorded. All of the experiments were carried out at room temperature unless otherwise specified.

3. Results and Discussion

3.1. Characterizations of the MB-MWNT Nanocomposite

It is well known that some aromatic dyes with polynuclear structure can easily adsorb onto the surface of CNTs through $\pi-\pi$ stacking forces between the two conjugated frames, forming new kinds of nanocomposites [5, 24]. Figure 1A showed the UV/Vis spectra of the MB solution, MWNT suspension and MB-MWNT nanocomposite suspension from 400 to 900 nm. The MB solution has two absorbance peaks at 615 nm and 665 nm (curve of Fig. 1A). Generally, the strong absorbance at 665 nm is the characteristic adsorption of MB monomers, and the shoulder at 617 nm is attributed to the absorbance of the MB dimer in solution [26]. No absorbance peaks for the MWNTs suspension were observed over this range (curve b of Fig. 1A). It can be observed that the MB-MWNT nanocomposite suspension shows a similar spectrum to that of the MB solution, but the absorbance is decreased (curve c of Fig. 1A). Compared with the MB solution at the same concentration, the decreased absorbance of the MB-MWNT nanocomposite suspension suggested that some free MB molecules in the suspension were deposited onto the surface of the MWNTs. Furthermore, the formation of MB-MWNT nanocomposites in the premixing suspension was investigated by SEM, as shown in Figure 1B. The MB-

MWNTs nanocomposites were adsorbed onto the silicon wafer under electrostatic forces. Compared with naked MWNTs, the surface of the MB-MWNTs became much rougher, suggesting that the MB molecules successfully deposited onto the surface of the MWNTs.

3.2. Characterization of (MB-MWNTs/HRP)$_n$ Multilayers

Schematic representations of the construction of the MB-MWNT nanocomposites and (MB-MWNTs/HRP)$_n$ multilayers were exhibited in Figure 2A. The cationic MB molecules adsorbed onto the negatively charged surface of MWNTs through a premixing process, and a MB-MWNT nanocomposite was constructed (process 1 of Fig. 2A). The net charge of MB-MWNTs nanocomposite was negative (-53 mV), as evaluated by zeta potentiometer detection. This finding might be attributed to the negative charges of the MWNTs exceeding the positive charges of the adsorbed MB with a weak cationic charge. On the other hand, with an isoelectric point of 7.2, the HRP molecules possessed a net positive charge in barbital-HCl buffer (pH 6.8). The alternative assembly was feasible under an electrostatic driving force. Process 2 shows the assembly procedure of (MB-

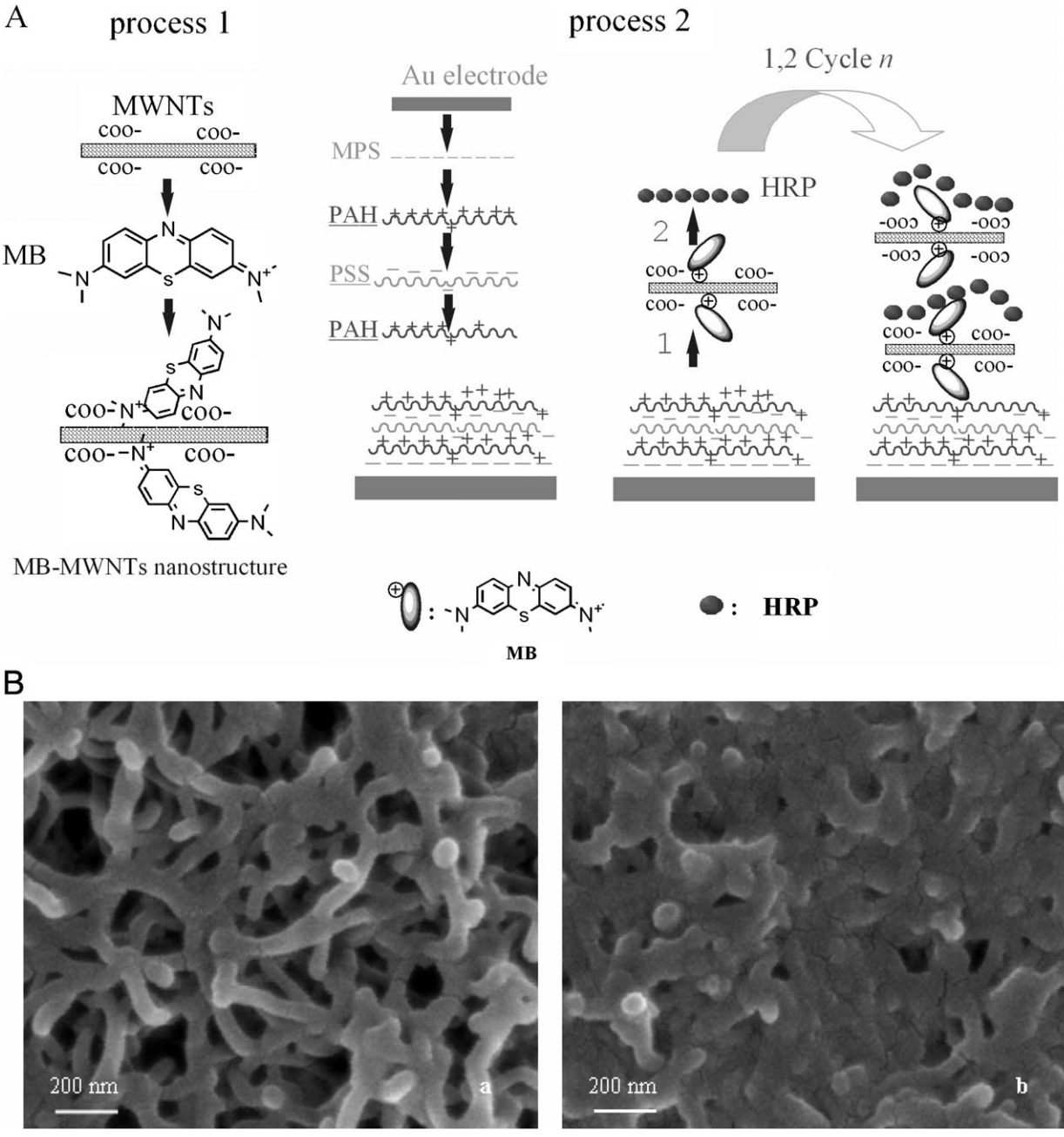

Fig. 2. A) The creation of MB-MWNTs nanocomposites by premixing and (MB-MWNTs/HRP)$_n$ multilayer assembly. B) SEM images of the outermost layer of the silicon wafers after LBL assembly of a) (MB-MWNTs/HRP)$_2$ (MB-MWNTs) and b) (MB-MWNTs/HRP)$_3$.

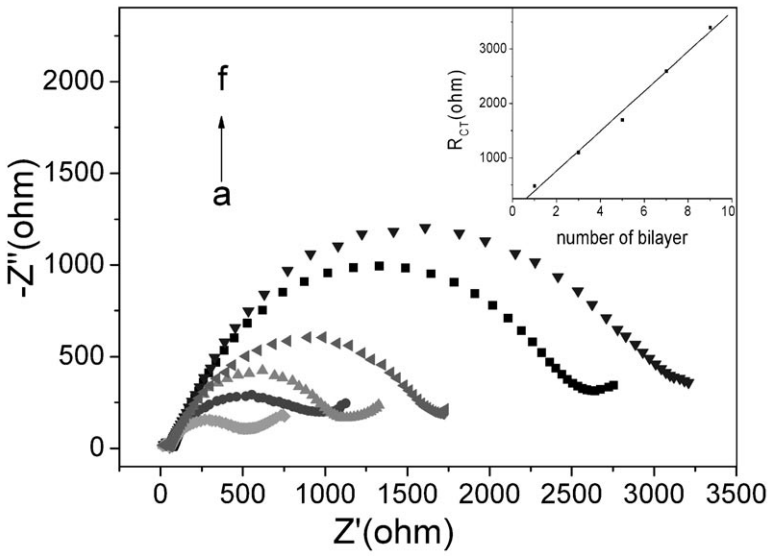

Fig. 3. Electrochemical impedance diagram for the electrode with different numbers of (MB-MWNTs/HRP) bilayers in 5.0 mM $K_3[Fe(CN)_6]/K_4[Fe(CN)_6]$ (1:1) solutions. a) $(MB\text{-}MWNTs/HRP)_1$ and c–f) 3, 5, 7, 9 bilayers. b) The same as (c) except with (MB-MWNTs) as the outermost layer. The inset shows the relationship of R_{ct} versus the number of bilayers.

$MWNTs/HRP)_n$ multilayers on precursor-modified Au electrodes. The morphology characteristics of the multilayers were investigated using SEM. After three bilayers of MB-MWNTs/HRP were assembled, the outermost of the multilayers was covered by a large amount of MB-MWNT nanocomposite with a rough surface (a of Fig. 2B). When the HRP became the outermost layer, the disappearance of part of the porous structure (b of Fig. 2B) implied that the MB-MWNTs nanocomposite could adsorb HRP molecules and act as a support matrix for the next assembly of HRP.

The LBL assembly process for the formation of $(MB\text{-}MWNTs/HRP)_n$ multilayers was also verified by electrochemical impedance spectrometry (EIS) [27]. EIS is an effective tool for investigating the origin of the electroactive membrane. EIS diagrams of electrodes modified with different numbers of MB-MWNTs/HRP bilayers ($n = 1$, 3, 5, 7, 9) are demonstrated in Figure 3 and presented as Nyquist plots (Z'' versus Z'). The R_{ct} (charge transfer resistance) of Au electrodes modified with one, three, five, seven and nine MB-MWNTs/HRP bilayers were estimated to be 450, 923, 1714, 2600 and 3461 Ω, respectively. It was observed in the inset of Figure 3 that the R_{ct} increased proportionally to the number of bilayers, verifying the origin of the uniform multilayer assembly on the surface of the electrode. Moreover, the addition of MWNTs to the electrode results in a remarkable decrease in the charge transfer resistance and the mass transfer impedance, according to a relative comparative study [28]. When the composite of the MB-MWNTs was located on the outermost layer of the electrode, the R_{ct} of the electrodes modified with $(MB\text{-}MWNTs/HRP)_3$/MB-MWNTs was lower than that of electrodes modified with $(MB\text{-}MWNTs/HRP)_3$. This finding further confirmed that the effect of the MWNTs is to decrease the resistance by facilitating the electron transfer on the surface of the electrode.

3.3. Electrochemical Properties of $(MB\text{-}MWNTs/HRP)_n$-Multilayer Modified Electrode

Cyclic voltammetry (CV) was performed to investigate the electrochemical behavior of the $(MB\text{-}MWNTs/HRP)_n$ mutilayers. Figure 4 shows the CV behavior of the different modified electrodes. No redox peak was found for the electrode modified by $(MWNTs/HRP)_3$ from -0.4 V to $+0.2$ V (Fig. 4a). When the $(MB/HRP)_3$ electrode was recycled in PBS buffer, a pair of well-defined redox peaks appeared at -0.25 V and -0.14 V due to the electron transfer between the immobilized MB and the electrode (Fig. 4b). This CV result was similar to that in previous research based on the LBL assembly of SWNTs and MB [24]. The ΔE_p of -0.11 V is relatively large, implying the sluggish process of electron transfer on the $(MB/HRP)_3$ electrode [29]. As for the $(MB\text{-}MWNTs/HRP)_3$ modified electrode, the reduction peak currents dramatically increased with a decrease in the oxidation peak current (Fig. 4c). The inset of Figure 4 shows the CV of the $(MB\text{-}MWNTs/HRP)_3$ electrode in the absence or presence of 0.5 mM H_2O_2. When H_2O_2 was added (solid line of inset), the reduction peak current of the $(MB\text{-}MWNTs/HRP)_3$ electrode increased with a decrease in the oxidation peak. The results indicate that a catalytic reaction occurred on this biosensor, and the response of the biosensor to H_2O_2 resulted from the catalytic activity of the immobilized HRP [11, 30]. Moreover, the immobilized MWNTs effectively enhanced the catalytic current response of the electrode.

In the case of $(MB\text{-}MWNTs/HRP)_3$ electrode, the reduction current dramatically increased with a decrease of the oxidation peak current in the absence of H_2O_2. However, no similar phenomenon was found in the electrode modified by $(MWNTs/HRP)_3$ or $(MB/HRP)_3$. As a probable explana-

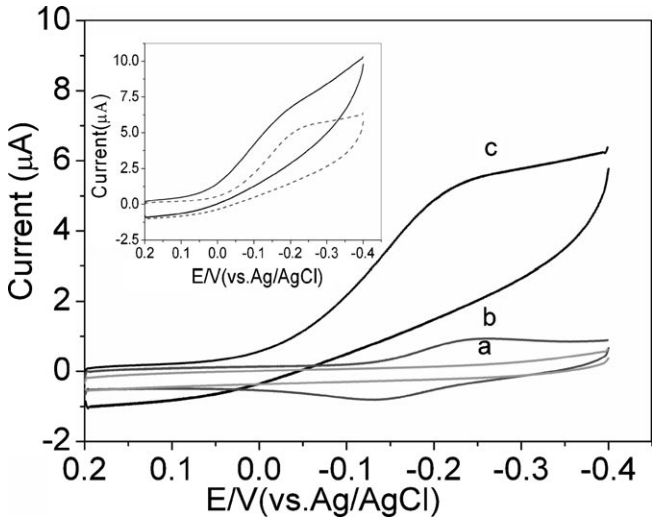

Fig. 4. Cyclic voltammograms of the electrodes modified by (a) $(MWNTs/HRP)_3$, (b) $(MB/HRP)_3$, or (c) $(MB\text{-}MWNTs/HRP)_3$. Inset: CV of $(MB\text{-}MWNTs/HRP)_3$ in the absence (dashed line) and presence (solid line) of 0.5 mM H_2O_2. All samples were in 0.1 M PBS at pH 6.8 and measured at a scan rate of 100 mV s^{-1}.

tion, MWNTs might interact with the MB, and the electrochemical active sites on MWNTs could probably have synergistic effect with electron mediator. The similar CVs profiles have also been reported [30, 31]. This kind of CVs behavior above will be worth investigating further.

3.4. Optimization of the Amperometric Experimental Conditions

The response of the biosensor was affected by the immobilization of the enzyme layer. The number of bilayers of MB-MWNTs/HRP on the modified biosensor was optimized. More (MB-MWNTs/HRP) bilayers can provide more electroactive species for catalytic reactions. When the number of bilayers increased from one to five, the amperometric response of the biosensor increased and reached a maximum at five bilayers. The amperometric signal decreased at six bilayers, probably because the film was too thick. The substrate diffusion was obstructed, and the action of the electron transfer rate was delayed [32, 33]. As a result, five bilayers of MB-MWNTs/HRP were chosen for further investigation.

Other factors were also investigated, including working potential, pH and concentration of electrochemical working buffer. The concentration of working buffer was investigated over a range of 0.05 to 0.4 M. The amperometric response increased from 0.05 M to 0.1 M and slowly decreased from 0.1 to 0.4 M, accompanied with an increase in response time. This finding was probably due to a higher concentration of buffer interfering with the enzymatic reaction [34]. Therefore, 0.1 M PBS was chosen as a working electrolyte throughout the experiments. The effect of pH from 5.0 to 9.0 was also evaluated. The current response of the biosensor reached the highest level at pH 6.8. The responses of the biosensor at different potentials ranged from +0.2 V to −0.4 V. At the applied potentials from +0.2 V to −0.2 V, the electroreduction response of H_2O_2 increased and reached a peak plateau between −0.2 V and −0.25 V. From −0.25 V to −0.4 V, the response of the electrode gradually decreased. Moreover, the baseline current of the signal became unstable above −0.25 V. As a result, −0.2 V was finally chosen as the applied potential throughout all the amperometric measurements.

3.5. Steady-State Amperometric Response of the Biosensor to Hydrogen Peroxide

Figure 5 gave the typical current–time curve of the $(MB\text{-}MWNTs/HRP)_5$ electrode in response to successive addition of different concentrations of H_2O_2 under stirring. Figure 5A is the amplification of a selected zone of Figure 5B. The biosensor could easily detect 4 μM H_2O_2, and it responded to H_2O_2 immediately and reached 95% of the steady-state current within 3 s. The fast response implied that the proposed biosensor could be extended into the flow system or other real time monitoring equipment.

The upper inset of Figure 5B compared the amperometric responses of the electrodes modified by $(MWNTs/HRP)_5$ (1 of upper inset), $(MB/HRP)_5$ (2 of upper inset) and $(MB\text{-}MWNTs/HRP)_5$ (3 of upper inset) during the addition of 200 μM H_2O_2. In comparison with the $(MB/HRP)_5$ electrode, the $(MWNTs/HRP)_5$ modified electrode without MB showed a very weak response to H_2O_2. However, the response of the $(MB\text{-}MWNTs/HRP)_5$ electrode was about three times higher than that of the $(MB/HRP)_5$ electrode. This result indicated that the MWNT matrix effectively enhanced the electrode signal in response to the substrate. This phenomenon was similar to the research conclusions based on the toluidine blue, MWNTs [7] and polythionine nanowire systems [35]. The MWNTs can adsorb enzymes during the construction of biosensors due to their inherent advantage of a large surface to volume ratio. Moreover, MWNTs can effectively improve the electron transfer due to their excellent conducting performance [36, 37]. Under the optimal conditions above, the linear range of the biosensor for the determination of H_2O_2 was evaluated from 4.0 μM to 3.78 mM with a sensitivity of 22.5 μA mM^{-1} and a correlation coefficient of 0.9996 (bottom inset of Fig. 5B). The detection limit of 1.0 μM was estimated at a signal-to-noise ratio of three.

The response of the enzyme-biosensor was also consistent with the Michaelis–Menten kinetic process of the enzyme catalytic reaction. The kinetic parameter of the amperometric detection of H_2O_2 was calculated. The K_m^{app} was evaluated by applying the results shown in Figure 5B to the electrochemical Michaelis–Menten equation [38].

$$i = I_{max} - K_m^{app}\,(i/C) \quad (1)$$

where i is the steady-state current, C is the concentration of H_2O_2, K_m^{app} is the apparent Michaelis–Menten constant,

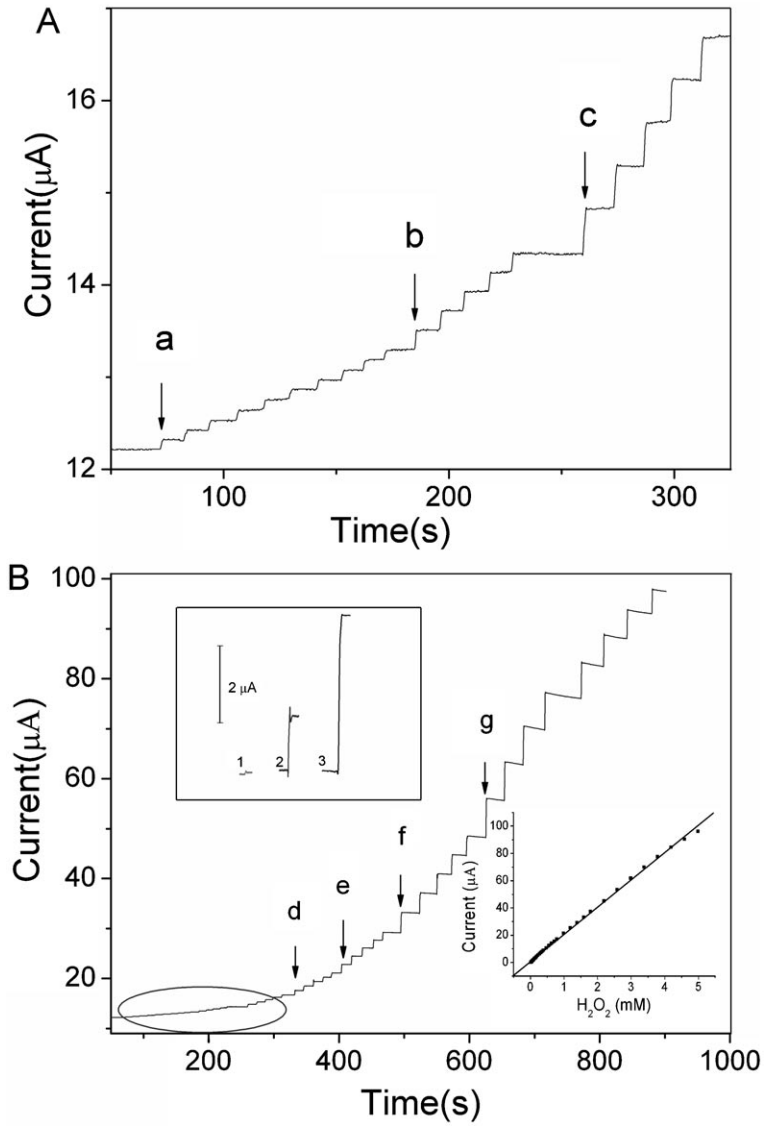

Fig. 5. A) The amperometric response of $(MB\text{-}MWNTs/HRP)_5$ modified electrodes to successive additions of a) 4.0 μM, b) 8.0 μM, and c) 20 μM H_2O_2. B) The electrochemical response of $(MB\text{-}MWNTs/HRP)_5$ modified electrodes to successive additions of d) 40 μM, e) 80 μM, f) 200 μM, and g) 400 μM H_2O_2. Upper inset: Comparison of the amperometric response of (1) $(MWNTs/HRP)_5$, (2) $(MB/HRP)_5$, and (3) $(MB\text{-}MWNTs/HRP)_5$ modified electrodes to 200 μM H_2O_2. Bottom Inset: calibration curve of the current response to the concentration of hydrogen peroxide. All experiments were completed in 0.1 M phosphate buffer at pH 6.8 at an operational potential of −0.20 V.

and I_{max} is the maximum current response. A good linear relationship was obtained between i^{-1} and C^{-1}, and the K_m^{app} value of the $(MB\text{-}MWNTs/HRP)_5$ electrode was 3.56 mM. The K_m^{app} value was markedly lower than that of the immobilized HRP in the sol-gel on the GCE ($K_m^{app} =$ 23.85 mM) [31]. It was also lower than that of the clay/AuCS-myoglobin based biosensor ($K_m^{app} = 5.1$ mM) [39]. This result suggested that the proposed electrode exhibited a high catalytic ability for H_2O_2. The biocompatibility of the assembled film maintained the high catalytic activity of HRP. A comparison to the analytical parameters of some reagentless H_2O_2 biosensors was exhibited in Table 1.

3.6. Interference Tests, Reproducibility and Stability of the Biosensor

Some possible interfering species, such as ascorbic acid, uric acid and glucose, were investigated to evaluate the anti-interference of the electrode. Figure 6 shows that the addition of 0.4 mM ascorbic acid, glucose and uric acid into an electrochemical cell containing 80 μM H_2O_2 did not produce observable interference. The low potential detection and the use of a mediator immobilized on the surface of the electrode allowed us to overcome the potential interferences [11, 40, 45, 46].

Table 1. Analytical parameters comparing the reagentless hydrogen peroxide biosensors. HRP: horseradish peroxidase; *LOD*: limit of detection; PTHNW: polythionine nanowires; SGCCN: sol-gel-derived ceramic–carbon nanotube; Mb: myoglobin; AuCS: Au nanoparticles-chitosan; Hb: hemoglobin; MCMS: magnetic chitosan microsphere; Bir: Birnessite; P123: poly(ethylene oxide)–poly(propylene oxide)–poly(ethylene oxide); MG: Methylene green.

Type of sensor construction	Detection potential (V)	K_m^{app} (mM)	*LOD* (μM)	Response time (s)	Reference
(MB–MWNTs/HRP)$_5$/PAH/PSS/PAH/Au	–0.2	3.56	1.0	<3	This work
Ti/TiO_2/Au/HRP	–0.6	–	2.0	<5	[30]
PTHNW–HRP/GC	–0.1	–	0.3	<5	[35]
HRP/SGCCN/GCE	–0.25	23.85	12.89	<4	[31]
clay–Mb–clay/AuCS–GCE	–0.26	5.10	7.5	–	[39]
Hb/MCMS/GCE	–0.2	–	21.0	<10	[40]
(MB–SiO_2)/HRP–gel/GCE	–0.3	0.9	4.0	<20	[41]
MB–Bir/HRP/GCE	–0.22	–	1.3	<8	[42]
Hb/P123/PG	–0.35	0.51	0.5	–	[43]
MWNTs/MG/HRP/GCE	–0.18	1.8	0.5	<10	[44]

The operational stability of the enzyme electrode was measured. The modified electrode presented with excellent repeatability with an *RSD* of 4.8% for a series of eight successive measurements of 0.2 mM H_2O_2. By comparison, the six electrodes prepared in the same fabrication procedure had a relative standard deviation of 5.8% with 0.2 mM H_2O_2. The storage stability of the biosensor was investigated by determining the steady-state response current of 0.2 mM H_2O_2 every week after preparation, the *RSD* of steady-state response current was 6.2%. When not in use, the biosensor was stored in 0.1 M PBS buffer at 4 °C. The results showed that the steady-state response current only decreased by 10% after 60 days, indicating that the enzyme electrode was considerably more stable than the reagentless biosensor based on the dropping or simple absorption method [11, 12].

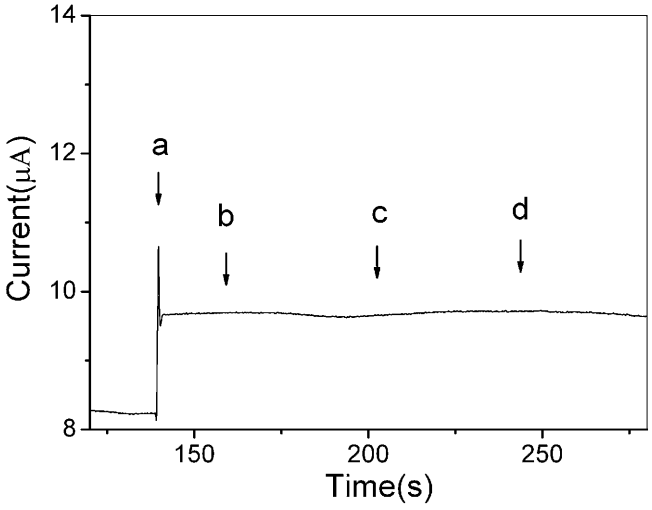

Fig. 6. The electrochemical response of the (MB-MWNTs/HRP)$_5$ modified electrode to successive additions of H_2O_2 and interferences of a) 80 μM H_2O_2, b) 0.4 mM ascorbic acid, c) 0.4 mM glucose, and d) 0.4 mM uric acid in 0.1 M phosphate buffer at pH 6.8 and at an applied potential of –0.20 V.

4. Conclusions

A uniform and stable multilayer membrane of MB-MWNT nanocomposites and enzymes can be constructed by a simple LBL assembly strategy. Under the mild environment of LBL assembly, MB-MWNT nanocomposites and HRP were alternately assembled using an electrostatic interaction on the surface of the Au electrode that was modified by precursors. The enzyme maintained its catalytic activity, and the MB-MWNTs nanocomposite showed electrochemical activity. The electrochemical response can be used for the determination of hydrogen peroxide. Several potential interfering factors were experimentally excluded. With this construction strategy, a reagentless biosensor can easily be fabricated. This LBL strategy extends the application of MB-MWNTs/electron mediator nanocomposites to the fabrication of amperometric biosensors.

5. Acknowledgements

Financial support from the National Natural Science Foundation of China (20805043, 30800247) is gratefully acknowledged.

6. References

[1] M. Janotta, F. Vogt, H. S. Voraberger, W. Waldhauser, J. M. Lackner, C. Stotter, M. Beutl, B. Mizaikoff, *Anal. Chem.* **2004**, *76*, 384.
[2] X. S. Chai, Q. X. Hou, Q. Luo, J. Y. Zhu, *Anal. Chim. Acta* **2004**, *507*, 281.
[3] Y. Xiao, H. X. Ju, H. Y. Chen, *Anal. Chim. Acta* **1999**, *391*, 299.
[4] Y. Xiao, H. X. Ju, H. Y. Cheng, *Anal. Biochem.* **2000**, *278*, 22.
[5] P. Du, B. Zhou, C. X. Cai, *J. Electroanal. Chem.* **2008**, *614*, 149.
[6] A. S. Santos, R. S. Freire, L. T. Kubota, *J. Electroanal. Chem.* **2003**, *547*, 135.
[7] Y. Liu, J. P. Lei, H. X. Ju,. *Talanta* **2008**, *74*, 965.
[8] S. H. Chen, R. Yuan, Y. Q. Chai, Na Li, *Electroanalysis* **2008**, *20*, 418.

[9] N. J. Sun, L. H. Guan, Z. J. Shi, N. Q. Li, Z. N. Gu, Z. W. Zhu, M. X. Li, Y. H. Shao, *Anal. Chem.* **2006**, *78*, 6050.
[10] S. L.P. Dias, S. T. Fujiwara, Y. Gushikem, R. E. Bruns, *J. Electroanal. Chem.* **2002**, *531*, 141.
[11] X. Q. Lin, J. Chen, Z. H. Che, *Electroanalysis* **2000**, *12*, 306.
[12] J. Z. Xu, J. J. Zhu, Q. Wu, Z. Hu, H. Y. Chen, *Electroanalysis* **2003**, *15*, 219.
[13] R. H. Baughman, A. Zakhidov, W. A. de Heer, *Science* **2002**, *297*, 787.
[14] J. Wang, M. Musameh, *Anal. Chem.* **2003**, *75*, 2075.
[15] A. C. Pereira, M. R. Aguiar, A. Kisner, *Sens. Actuators B, Chem.* **2007**, *124*, 269.
[16] H. B. Shi, Y.Yang, J. D. Huang, Z. X. Zhao, X. H. Xu, J. Anzai, T. Osa, Q. Chen, *Talanta* **2006**, *70*, 852.
[17] X. Chen, Y. Yang, M. Y. Ding, *Anal. Chim. Acta* **2006**, *557*, 52.
[18] G. D. Liu, Y. H. Lin, *Electrochem. Commun*. **2006**, *8*, 251.
[19] R. Z. Ma, T. Sasaki, Y. Bando, *J. Am. Chem. Soc.* **2004**, *126*, 10382.
[20] C. Tedeschi, L. D. Li, H. Mohwald, C. Spitz, D. V. Seggern, R. Menzel, *J. Am. Chem. Soc.* **2004**, *126*, 3218.
[21] A. A. Mamedov, N. A. Kotov, M. Prato, D. M. Guldi, J. P. Wicksted, A. Hirsch, *Nat. Mater.* **2002**, *1*, 190.
[22] H. T. Zhao, H. X. Ju, *Anal. Biochem.* **2006**, *350*, 138.
[23] Y. J. Zou, C. L. Xiang, L. X. Sun, F. Xu, *Electrochim. Acta* **2008**, *53*, 4089.
[24] Y. M. Yan, M. N. Zhang, K. P. Gong, L. Su, Z. X. Guo, L. Q. Mao, *Chem. Mater.* **2005**, *17*, 3457.
[25] L. J. Liu, F. Zhang, F. N. Xi, X. F. Lin, *Biosens. Bioelectron.* **2008**, *24*, 306.
[26] T. Sagara, K. Niki, *Langmuir* **1993**, *9*, 831.
[27] E. Katz, L. Alfonta, I. Willner, *Sens. Actuators B, Chem.* **2003**, *76*, 134.
[28] S. Carrara, V. Bavastrello, D. Ricci, E. Stura, C. Nicolini, *Sens. Actuators B, Chem.* **2005**, *109*, 221.
[29] S. Chakraborty, C. R. Raj, *Electrochem. Commun.* **2007**, *9*, 1323.
[30] A. K.M. Kafi, G. S. Wu, A. C. Chen, *Biosens. Bioelectron.* **2008**, *24*, 566.
[31] H. Chen, S. Dong, *Biosens. Bioelectron.* **2007**, *22*, 1811.
[32] P. Du, S. N. Liu, P. Wu, C. X. Cai, *Electrochim. Acta* **2007**, *53*, 1811.
[33] F. Bellezza, A. Cipiciani, U. Costantino, M. E. Negozio, *Langmuir* **2002**, *18*, 8737.
[34] C. F. Nan, Y. Zhang, G. M. Zhang, C. Dong, S. M. Shuang, M. M. F. Choi, *Enzyme Microb. Tech.* **2009**, *44*, 249.
[35] A. W. Shi, F. L. Qu, M. H. Yang, G. L. Shen, R. Q. Yu, *Sens. Actuators B, Chem.* **2008**, *129*, 779.
[36] P. J. Britto, K. S. V. Santhanam, V. Alonso, A. Rubio, P. M. Ajayan, *Adv. Mater.* **1999**, *11*, 154.
[37] G. A. Rivas, M. D. Rubianes, M. C. Rodríguez, N. F. Ferreyra, G. L. Luque, M. L. Pedano, S. A. Miscoria, C. Parradov, *Talanta* **2007**, *74*, 291.
[38] R. A. Kamin, G. S. Wilson, *Anal. Chem.* **1980**, *52*, 1198.
[39] X. J. Zhao, Z. B. Mai, X. H. Kang, *Electrochim. Acta* **2008**, *53*, 4732.
[40] G. S. Lai, H. L. Zhang, D. Y. Hana, *Sens. Actuators B, Chem.* **2008**, *129*, 497.
[41] H. Yao, N. Li, S. Xu, J. Z. Xu, J. J. Zhu, H. Y. Chen, *Biosens. Bioelectron.* **2005**, *21*, 372.
[42] X. S. Yang, X. Chen, X. Zhang, W. S. Yang, D. G. Evans, *Sens. Actuator B, Chem.* **2008**, *129*, 784.
[43] N. Q. Jia, Q. Lian, Z. Y. Wang, H. B. Shen, *Sens. Actuators B. Chem.* **2009**, *137*, 230.
[44] A. K. Upadhyay, T. W. Ting, S. M. Chen, *Talanta* **2009**, *79*, 38.
[45] C. X. Lei, S. Q. Hu, N. Gao, G. L. Shen, R. Q. Yu, *Bioelectrochemistry* **2004**, *65*, 33.
[46] G. Wang, J. J. Xu, H. Y. Chen, Z. H. Lu, *Biosens. Bioelectron*. **2003**, *18*, 335.

